Density distribution in two Ising systems with particle exchange

Jean-Yves Fortin, Segun Goh, Chansoo Kim, Mooyoung Choi

Density distribution in two Ising systems with particle exchange

Jean-Yves Fortin[1], Segun Goh[2], Chansoo Kim[3,4], MooYoung Choi[5]

[1]Laboratoire de Physique et Chimie Théoriques, CNRS UMR 7019,
Université de Lorraine, 54506 Vandoeuvre-lès-Nancy, France

E-mail: jean-yves.fortin@univ-lorraine.fr
[2]Institut für Theoretische Physik II: Weiche Materie,
Heinrich-Heine-Universität Düsseldorf, D-40225 Düsseldorf, Germany
[3]Center for Computational Science and Social and Economic Engineering Initiative,
Korea Institute of Science and Technology, Seoul 136-791, South Korea
[4]Department of Economics and Institute for Research in Finance & Economics, Seoul National University, Seoul 151-742, South Korea
[5]Department of Physics and Center for Theoretical Physics,
Seoul National University, Seoul 151-747, South Korea

E-mail: mychoi@snu.ac.kr

Abstract. Various physical and social systems are subject to exchanges of their constituent particles, in addition to usual energy exchanges or fluctuations. In this paper we consider a system consisting of two Ising systems, a one-dimensional lattice (solid) and a fully connected system (gas) or reservoir (with constant fugacity), and exchanging particles between the two, and study the exact distribution of particles as a function of the internal couplings, temperature, and external field. Particles (with spins) in the gas can be adsorbed onto the one-dimensional lattice (corresponding to condensation) or desorbed back into the reservoir (evaporation). The distribution of the number of particles on the lattice is computed exactly and the thermodynamic limit is studied by means of the saddle-point analysis. It is found that the probability follows a cumulative Gumbel distribution, with the argument proportional to the free energy cost of removing one site.

PACS numbers: 05.50.+q,64.60.De,75.10.Hk,05.70.Fh

1. Introduction

In typical statistical models, numbers of particles are supposed to be conserved and properties depend only on internal energy exchange, which in many cases leads to various phase transitions [1, 2]. However, important phase properties of physical systems depend on particle or material exchange between subsystems, for example between solids and gases by surface evaporation or catalysis [3, 4], or between Bose condensates and environments [5, 6], where the number of particles is not conserved. There are different ways of introducing interactions in these models. External currents can also play the role of a particle reservoir injected in the system [7, 8], while catalysis or coagulation phenomena removes particles [9, 10]. In many cases, it is relevant to study how particle exchange processes affect the equilibrium distribution of particles in a given system, as a function of external parameters such as the temperature or external magnetic field. Transfer processes in social networks are often described by flow of their constituents [11], which may be modeled by non-conservative master equations. Here we study flow of particles due to local energy fluctuations depending on whether the transfer is energetically favorable or not. When the temperature is high, particles tend to evaporate into the gas; at low temperatures particles tend to aggregate into an ordered configuration on a lattice and this configuration is selected. We expect that, as the number of particles grows, the asymptotic behavior of the concentration distribution displays universal behavior at equilibrium.

In this paper, we consider two Ising systems, one on a one-dimensional lattice with local interactions and the other being fully connected, in contact with each other. There are no inter-system interactions between particles but only inter-system exchanges of particles, namely, particles in one system do not interact with those in the other but they are subject to direct exchange between the two systems. In an earlier paper [12], we studied the effects of particle exchange on the physical properties between two fully connected Ising systems, and proved specifically the existence of additional stable phase transitions. Here we want to study how the distribution of particles or clusters of particles behaves in the one-dimensional lattice considered as a solid. This problem is exactly solvable with a saddle point analysis and information on the size-dependent distribution is obtained in the asymptotic limit. In particular, we give exact results for the cluster size distribution in two scaling limits, when the one-dimensional lattice is partially or fully occupied.

This paper consists of five sections: In section 2, we describe the model in detail, and compute the partition function. The distribution of particles on the lattice is then defined and studied in section 3. In particular, a saddle-point analysis allows us to take the thermodynamic limit of the system. Effects of an external field are described subsequently. In section 4, we consider the case that the other system is specified by constant fugacity, namely, we investigate the one-dimensional lattice system in contact with a (heat and particle) reservoir. Finally, section 5 summarizes the results whereas two Appendices present details of calculations.

2. Model Hamiltonian

We consider spin particles interacting via Ising couplings within one of the two systems, a one-dimensional (1D) system $\mathcal{S}_{1D}$ and a fully-connected system $\mathcal{S}_C$. The two systems $\mathcal{S}_{1D}$ and $\mathcal{S}_C$ are not coupled directly but transfer of particles is allowed between $\mathcal{S}_{1D}$ and $\mathcal{S}_C$, which induces indirect correlations via this particle exchange, and the total number of particles N is conserved. The intrinsic coupling constants in $\mathcal{S}_{1D}$ and in $\mathcal{S}_C$ are given by J and J_0, respectively, and particles in $\mathcal{S}_{1D}$ are subjected to an external field h_e. The total Hamiltonian can be written in terms of spin variables $\sigma_i = \pm 1$ and occupation numbers $\rho_i = 0, 1$:

$$H = -J\sum_{i=1}^{N}\rho_i\rho_{i+1}\sigma_i\sigma_{i+1} - \frac{J_0}{2N}\sum_{i,j\geq 1}^{N}(1-\rho_i)(1-\rho_j)\sigma_i\sigma_j - h_e\sum_{i=1}^{N}\rho_i\sigma_i \tag{1}$$

where $\rho_i = 1$ for spin particle σ_i located in the 1D system $\mathcal{S}_{1D}$ and $\rho_i = 0$ for σ_i located in the fully-connected system $\mathcal{S}_C$. We first consider the partition function for the N particles:

$$Z_0 = \mathrm{Tr}_{\{\rho_i,\sigma_i\}}\exp\left[K\sum_{i=1}^{N}\rho_i\rho_{i+1}\sigma_i\sigma_{i+1} + \frac{K_0}{2N}\sum_{i,j\geq 1}^{N}(1-\rho_i)(1-\rho_j)\sigma_i\sigma_j + h\sum_{i=1}^{N}\rho_i\sigma_i\right] \tag{2}$$

with $K \equiv J/T$, $K_0 \equiv J_0/T$, and $h \equiv h_e/T$ at temperature T. Open boundary conditions are taken for the 1D system. Via a Hubbard-Stratonovich transformation, one obtains the partition function in the form

$$\begin{aligned} Z_0 = \int_{-\infty}^{\infty}\mathrm{d}y\sqrt{\frac{NK_0}{2\pi}}\mathrm{Tr}_{\{\sigma_i,\rho_i\}}\exp\Bigg[-\frac{1}{2}NK_0y^2 + K\sum_{i=1}^{N}\rho_i\rho_{i+1}\sigma_i\sigma_{i+1} \\ +K_0y\sum_{i=1}^{N}(1-\rho_i)\sigma_i + h\sum_{i=1}^{N}\rho_i\sigma_i\Bigg]. \end{aligned} \tag{3}$$

It is convenient to express the partition function as an expansion of $\mathcal{S}_{1D}$ clusters. For this purpose, we consider the configuration of k clusters of spins, represented by $\{n_1, \cdots, n_k\}$ with $n_i\,(\geq 1)$ being the size of the ith cluster, residing in system $\mathcal{S}_{1D}$, and the remaining $N - \sum_{i=1}^{k} n_k$ particles located in system $\mathcal{S}_C$. See Fig. 1 for a typical example. Each configuration $\{n_i\}$ is weighted with the factor $W_{n_1}W_{n_2}\cdots W_{n_k}V^{N-\sum_i n_i}$, where $V \equiv 2\cosh(K_0y)$ and $W_n \equiv r_+\lambda_+^{n-1} + r_-\lambda_-^{n-1}$ (see Appendix Appendix A for details as well as the explicit expressions of $r_\pm$ and $\lambda_\pm$). In the absence of the field

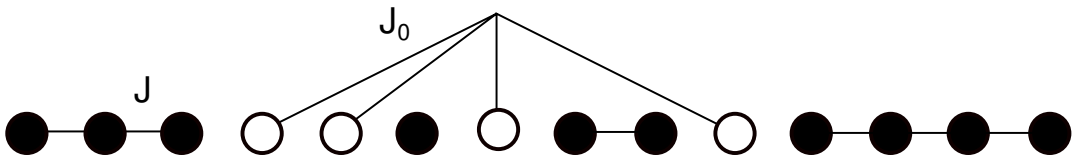

Figure 1. Exemplary configuration of $k = 4$ clusters of size $\{n_1, n_2, n_3, n_4\} = \{3, 1, 2, 4\}$. Filled and empty circles depict particles in $\mathcal{S}_{1D}$ ($\rho_i = 1$) and in $\mathcal{S}_C$ ($\rho_i = 0$), respectively.

($h = 0$), one has simply $W_n = 2^n \cosh^{n-1} K$. There is also a combinatorial factor associated with the fact that the clusters can be distributed along different positions in space. The general form of the partition function thus reads

$$Z_0 = \int_{-\infty}^{\infty} \mathrm{d}y \sqrt{\frac{NK_0}{2\pi}} \exp\left[-\frac{1}{2} NK_0 y^2\right] \Omega(y) \tag{4}$$

where

$$\begin{aligned}\Omega(y) &= V^N + \sum_{n_1=1}^{N} \tbinom{N-n_1+1}{N-n_1} W_{n_1} V^{N-n_1} + \sum_{n_1,n_2\geq 1}^{n_1+n_2\leq N-1} \tbinom{N-n_1-n_2+1}{N-n_1-n_2-1} W_{n_1} W_{n_2} V^{N-n_1-n_2} + \cdots \\ &= \sum_{k=0}^{(N+1)/2} \Omega_k(y). \end{aligned} \tag{5}$$

The first term $\Omega_0 \equiv V^N$ in Eq. (5) represents the empty state in $\mathcal{S}_{1D}$, whereas the second term Ω_1 describes those configurations with single clusters of all sizes. The last term $\Omega_{(N+1)/2}$ corresponds to the configuration of every other site occupied with one particle in $\mathcal{S}_{1D}$. Note that clusters do not touch each other and are separated by at least one empty site. Accordingly, the cluster size is bounded by $k \leq \sum_{i=1}^{k} n_i \leq N - k + 1$. To perform the sum over different configurations $\{n_i\}$, we define $s \equiv \sum_{i=1}^{k} n_i$, and write

$$\begin{aligned}\Omega_k(y) &= \sum_{n_1,n_2,\cdots,n_k\geq 1}^{n_1+n_2+\cdots+n_k\leq N-k+1} \tbinom{N-n_1-n_2-\cdots-n_k+1}{N-n_1-n_2-\cdots-n_k-k+1} \times W_{n_1} W_{n_2} \cdots W_{n_k} V^{N-n_1-n_2-\cdots-n_k} \\ &= \sum_{s=k}^{N-k+1} \tbinom{N-s+1}{N-s-k+1} V^{N-s} \sum_{n_1,n_2,\cdots,n_k\geq 1} W_{n_1} W_{n_2} \cdots W_{n_k} \delta_{s,n_1+\cdots+n_k} \\ &= \sum_{s=k}^{N-k+1} \tbinom{N-s+1}{N-s-k+1} V^{N-s} \omega_k(s) \end{aligned} \tag{6}$$

where $\omega_k(s)$ is the weight containing all the k-cluster configurations in $\mathcal{S}_{1D}$. In Ω_k, the only dependence on y comes from the term V^{N-s}, which reduces the integral over y in Eq. (4) to a finite sum:

$$z_N(s) = \int_{-\infty}^{\infty} \mathrm{d}y \sqrt{\frac{NK_0}{2\pi}} \exp\left[-\frac{1}{2} NK_0 y^2\right] V^{N-s} = \sum_{k=0}^{N-s} \tbinom{N-s}{k} \mathrm{e}^{-K_0(2k-N+s)^2/2N}$$

with $z_N(N) = 1$. The above representation of z_N in terms of the discrete sum is useful for numerical analysis. This leads to the partition function in the form

$$Z_0 = z_N(0) + \sum_{k=1}^{(N+1)/2} \sum_{s=k}^{N-k+1} \tbinom{N-s+1}{N-s-k+1} \omega_k(s) z_N(s) \tag{7}$$

where the first term corresponds to the contribution of the empty state in $\mathcal{S}_{1D}$ or of the all-occupied state in $\mathcal{S}_C$. Here $\omega_k(s)$, which includes the Kronecker delta constraining the total size of the k clusters to equal s, can be computed through the use of the following representation in the complex plane:

$$\omega_k(s) = \sum_{n_1,n_2,\cdots,n_k\geq 1} W_{n_1} W_{n_2} \cdots W_{n_k} \delta_{s,n_1+\cdots+n_k} = \oint \frac{\mathrm{d}z}{2i\pi z} z^s \left(\sum_{n=1}^{\infty} z^{-n} W_n\right)^k . \tag{8}$$

The series inside the integral converges only when the integral path encloses the two eigenvalues $\lambda_\pm$, namely, when $|\lambda_\pm/z| < 1$. The rather cumbersome expression for $\omega_k(s)$ is given by Eq. (A.5) in Appendix A, and is expressed in terms of discrete sums. In the absence of the external field, $\omega_k(s)$ takes a simple form and is given by

$$\omega_k(s) = \binom{s-1}{k-1} 2^s \cosh^{s-k} K \tag{9}$$

for $k \geq 1$.

3. Cluster Size Distribution

In this section we investigate the normalized distribution $p(n)$ of the cluster size, defined by the average of $k^{-1}\sum_{i=1}^{k}\delta_{n,n_i}$ for each configuration of k clusters:

$$\begin{aligned} p(0) &= \frac{\langle \Omega_0 \rangle_y}{\left\langle \sum_{k\geq 0} \Omega_k(y) \right\rangle_y} \\ p(n{\geq}1) &= \frac{\left\langle \sum_{k\geq 1} \Omega_k(y) k^{-1} \sum_{i=1}^{k} \delta_{n,n_i} \right\rangle_y}{\left\langle \sum_{k\geq 0} \Omega_k(y) \right\rangle_y} \end{aligned} \tag{10}$$

where the bracket denotes the average taken over y with the Gaussian weight in Eq. (4):

$$\langle F(y) \rangle_y \equiv \sqrt{\frac{NK_0}{2\pi}} \int \mathrm{d}y \exp\left(-\frac{1}{2} N K_0 y^2\right) F(y).$$

Taking into account the constraint that one of n_i's is equal to n, we compute the combinatorial coefficient associated with the configuration $\{n_i\}$, and obtain

$$\sum_{\{n_i\}} W_{n_1} W_{n_2} \cdots W_{n_k} \delta_{s,n_1+\cdots+n_k} \left(\frac{1}{k}\sum_{i=1}^{k} \delta_{n,n_i}\right) = W_n\, \omega_{k-1}(s{-}n), \tag{11}$$

which is correct for $k \geq 2$. For the one-cluster contribution $k = 1$, we instead have $\delta_{s,n} W_n$. As a result, the distribution reads, for $n \geq 1$,

$$p(n) = \frac{W_n}{Z_0}\left[(N-n+1) z_N(n) + \sum_{k=2}^{[(N-n+2)/2]} \sum_{s=k+n-1}^{N-k+1} \binom{N-s+1}{N-s-k+1} z_N(s) \omega_{k-1}(s{-}n)\right] \tag{12}$$

and $p(N) = W_N/Z_0$ for the maximum occupancy. In particular, in the absence of the external field, we have

$$\begin{aligned} p(n) = \Bigg\langle & \frac{N-n+1}{\cosh K} \frac{\cosh^n K}{\cosh^n(K_0 y)} \\ & + \sum_{k=2}^{[(N-n+2)/2]} \frac{1}{\cosh^k K} \sum_{s=n+k-1}^{N-k+1} \tbinom{N-s+1}{N-s-k+1} \tbinom{s-n-1}{k-2} \frac{\cosh^s K}{\cosh^s(K_0 y)} \Bigg\rangle_y \\ \Bigg/ & \left\langle 1 + \sum_{k=1}^{(N+1)/2} \frac{1}{\cosh^k K} \sum_{s=k}^{N-k+1} \tbinom{N-s+1}{N-s-k+1} \tbinom{s-1}{k-1} \frac{\cosh^s K}{\cosh^s(K_0 y)} \right\rangle_y . \end{aligned} \tag{13}$$

3.1. Saddle-point analysis

In the thermodynamic limit ($N \to \infty$), we introduce continuous variables $x = n/N$, $u = k/N$, and $v = s/N$, in order to transform the different finite sums in Eq. (13) into integrals. The binomial coefficients involved in Eq. (13) can be expressed as gamma functions, which reduce in the large-N limit to continuous functions of x, u, and v, as shown in Appendix Appendix B. Combining those terms, one can express the distribution as a ratio of triple integrals over y, u, and v:

$$p(n) = \frac{\int_{-\infty}^{\infty} \mathrm{d}y \int_0^{(1-x)/2} \mathrm{d}u \int_{u+x}^{1-u} \mathrm{d}v \, \mathrm{e}^{NS_0(x)} \frac{u(1-v)^{3/2}}{(v-x)^{1/2}(v-u-x)^{3/2}(1-u-v)^{3/2}}}{\int_{-\infty}^{\infty} \mathrm{d}y \int_0^{1/2} \mathrm{d}u \int_u^{1-u} \mathrm{d}v \, \mathrm{e}^{NS_0(0)} \frac{(1-v)^{3/2}}{v^{1/2}(v-u)^{1/2}(1-u-v)^{3/2}}} \tag{14}$$

where the action $S_0(x)$ is given by

$$\begin{aligned} S_0(x) &= -\frac{1}{2}K_0 y^2 + \ln[2\cosh(K_0 y)] - u \ln\cosh K \\ &+ v \ln\left[\frac{\cosh K}{\cosh(K_0 y)}\right] - 2u \ln u + (v-x)\ln(v-x) \\ &+ (1-v)\ln(1-v) - (v-u-x)\ln(v-u-x) \\ &- (1-u-v)\ln(1-u-v). \end{aligned} \tag{15}$$

For large N, one can use the saddle-point method to find the maximum S_0^* of S_0 by solving $\partial S_0/\partial y = \partial S_0/\partial u = \partial S_0/\partial v = 0$. This leads to the set of equations for u^*, v^*, and y^* corresponding to S_0^*:

$$\begin{aligned} u^* &= \frac{\lambda_0(1-\lambda_0-x)[\cosh K - \cosh(K_0 y^*)]}{(1-\lambda_0-x)\cosh K - \lambda_0 \cosh(K_0 y^*)} \\ v^* &= 1-\lambda_0 \end{aligned} \tag{16}$$

with $\lambda_0 \equiv y^*/\tanh(K_0 y^*)$, while y^* satisfies the implicit equation

$$\begin{aligned} &\lambda_0(1-\lambda_0-x)(\cosh K - 1)[\cosh K - \cosh(K_0 y^*)]^2 \\ &= [(1-\lambda_0-x)\cosh(K_0 y^*) - \lambda_0 \cosh K] \\ &\times [(1-\lambda_0-x)\cosh K - \lambda_0 \cosh(K_0 y^*)]\,. \end{aligned} \tag{17}$$

Note that the saddle-point equations are symmetric under $y^* \to -y^*$. Solutions y^* of Eq. (17), depending on the coupling constants K and K_0, are illustrated in Fig. 2.

We first probe the phase transition by analyzing the bifurcations of solutions y^*. The critical transition for the spin order in the fully-connected system $\mathcal{S}_C$, governed by y^*, depends on the value of v^* [see Eq. (15)]. If v^* is close to unity, the transition to the ordered phase (where y^* becomes nonzero) occurs at a very large value of $K_0 \approx 1/(1-v^*)$ ($\gg 1$). In the paramagnetic (disordered) sector $y^* = 0$, the saddle-point equation (for $x = 0$) is given by

$$\cosh K = \frac{(v^*-u^*)(1-u^*-v^*)}{u^{*2}} = \frac{(1-v^*)(v^*-u^*)}{v^*(1-u^*-v^*)} \tag{18}$$

which bears the solution

$$u^* = \frac{2}{\sqrt{(\cosh K - 1)^2 + 4}\left[\cosh K + 1 + \sqrt{(\cosh K - 1)^2 + 4}\right]}$$

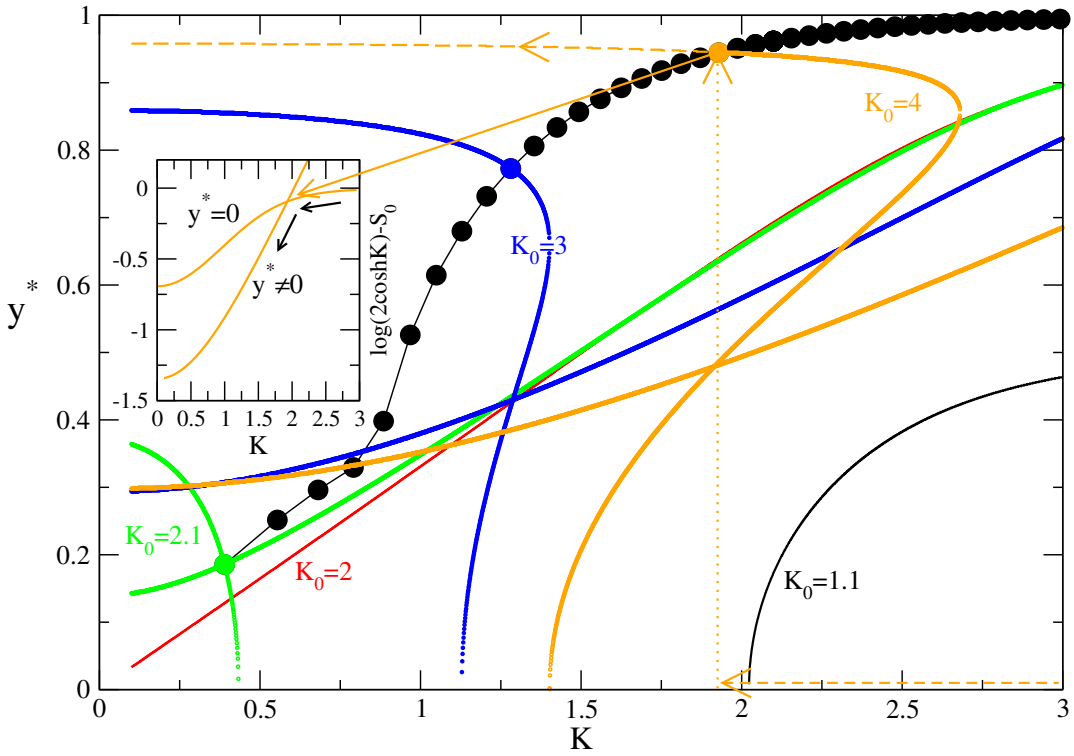

Figure 2. Diagram of the solutions y^* in Eq. (17) as function of K for various values of K_0 (with x set equal to 0). For $K_0 \leq 2$, there exists only one solution which is not stable; for $K_0 > 2$, two or three solutions are found, shown in different colors. In the first case ($K_0 \leq 2$) the saddle-point solution is given only by $y^* = 0$ and u^* and v^* by Eq. (19). For $K_0 > 2$ and K below the critical value K_c (indicated by the line of filled circles), the saddle-point solution is given by Eq. (16) and Eq. (17), for which S_0 is larger than the solution given by Eq. (19) (see the inset for $K_0 = 4$). For $K \geq K_c$, the solution is still given by $y^* = 0$ and Eq. (19). The line of filled circles plots the critical values K_c corresponding to different values of K_0, from 2.1 to 6 at the increment of 0.1. When $K_0 > 2$ and $K < K_c$, y^* is given by the largest of the two or three solutions which approaches unity as $K \to 0$ and $K_0 \gg 1$. The orange dashed line illustrates how the value of y^* for $K_0 = 4$ changes as K is lowered from $K = 3$. When K crosses the value $K = K_c \approx 1.915$ from above, y^* jumps from zero (dotted orange line), to the value given by the largest solution (top orange dashed line).

$$v^* = \frac{1}{2}\left[1 + \frac{\cosh K - 1}{\sqrt{(\cosh K - 1)^2 + 4}}\right]. \tag{19}$$

Note that for $K = 0$ solutions are simply given by $u^* = 1/4$ and $v^* = 1/2$. As K is decreased from the paramagnetic sector $y^* = 0$, there occurs a transition at which the solution of Eqs. (16)-(17) leads to a larger value of S_0. In Fig. 2, this happens at the locations (K_c, y^*) represented by the filled circles, depending on K_0. When three solutions exist ($K_0 \gtrsim 2.5$), this corresponds to the higher value of the y^* solution of Eq. (17) for which the saddle point is stable (as manifested by the fact that both eigenvalues of S_0'' are negative). When there are only two solutions ($K_0 \lesssim 2.5$), the critical point K_c is located at the crossing point between the two curves given

by $y^* = K_c/K_0$, which has been confirmed numerically. Indeed an obvious solution of Eq. (17) is given by $y^* = K/K_0$, for which the equation factorizes into $(1-2\lambda_0)^2 = 0$, corresponding to the crossing of the curves. In this case one obtains $u^* = 0, v^* = 1/2$, and $K_c = \frac{1}{2}K_0 \tanh K_c$, which is the implicit equation of K_c as function of K_0. The solution disappears for $K_0 < 2$, below which only one unstable solution $y^* \neq 0$ is found. In that case the solution is given by Eq. (18) at $y^* = 0$. In this manner the fully-connected system exhibits a first-order transition, characterized by a jump from $y^* = 0$ to a finite value.

We next examine the possibility of a phase transition in the 1D system $\mathcal{S}_{1D}$. Appendix A presents the exact form of the partition function Z_0 in the presence of the field. The spin order parameter, i.e., the magnetization of the system, which is defined to be $m \equiv \langle \sum_i \rho_i \rangle^{-1} \langle \sum_i \rho_i \sigma_i \rangle$, can easily be obtained from the derivative $\partial Z_0/\partial h$. It is then straightforward to show that Eq. (A.4) leads to $\lim_{h\to 0} \partial r_\pm/\partial h = 0$ and $\lim_{h\to 0} \partial \lambda_\pm/\partial h = 0$. In consequence we have $\langle \sum_i \rho_i \sigma_i \rangle = 0$, which confirms that the symmetry associated with the spin order does not break spontaneously in $\mathcal{S}_{1D}$ like the conventional 1D Ising model [13].

3.2. Probability for maximum occupancy

Returning to the cluster size distribution $p(n)$, we use Eq. (12) to compute $p(n{\geq}1)$ in the system of $N = 100$ particles, and plot the results in Fig. 3 for $K_0 = 5$ and various values of K. Manifested is an apparent transition between two states: one state where all sites in $\mathcal{S}_{1D}$ are mainly occupied (for $K \gtrsim 2$) and the other where the sites are sparsely occupied (for $K \lesssim 1.5$) with the distribution decaying fast. In the latter case, an exponential distribution is observed when K is low, whereas a flat distribution is obtained for sufficiently large K. There remains a question as to the nature of this behavior, which is analyzed below in the large-N limit. Moreover, the distribution $p(n)$ shows different forms in the two scaling limits $n \ll N$ (system sparsely filled) and $n \simeq N$ (system almost entirely filled). We therefore study separately the two limits and give the general results.

Given a solution (u^*, v^*, y^*) of the saddle-point equation (16) and (17), the distribution $p(n)$ in the limit $n \ll N$ takes the form

$$p(n{\ll}N) \approx \frac{u^*}{v^* - u^*} \exp\left[-n \ln\left(\frac{v^*}{v^* - u^*}\right)\right] \tag{20}$$

which decreases exponentially with the characteristic interval $n_c = \ln^{-1}(\frac{v^*}{v^*-u^*})$, as shown in Fig. 3. On the other hand, the probability that the whole system $\mathcal{S}_{1D}$ is filled with particles is given by

$$\begin{aligned} p(N) \approx{}& \frac{\sqrt{v^*(v^* - u^*)}}{\cosh K} \left(\frac{1 - u^* - v^*}{1 - v^*}\right)^{3/2} \\ & \times \sqrt{\mathrm{Det}(-S_0'')} \exp\left(N[\ln(2\cosh K) - S_0^*(0)]\right) \end{aligned} \tag{21}$$

where S_0'' is the Hessian matrix associated with S_0. The maximum $S_0^*(0)$ is calculated over the finite interval of integration in Eq. (14). For large K, we simply have $u^* \approx 0$ and

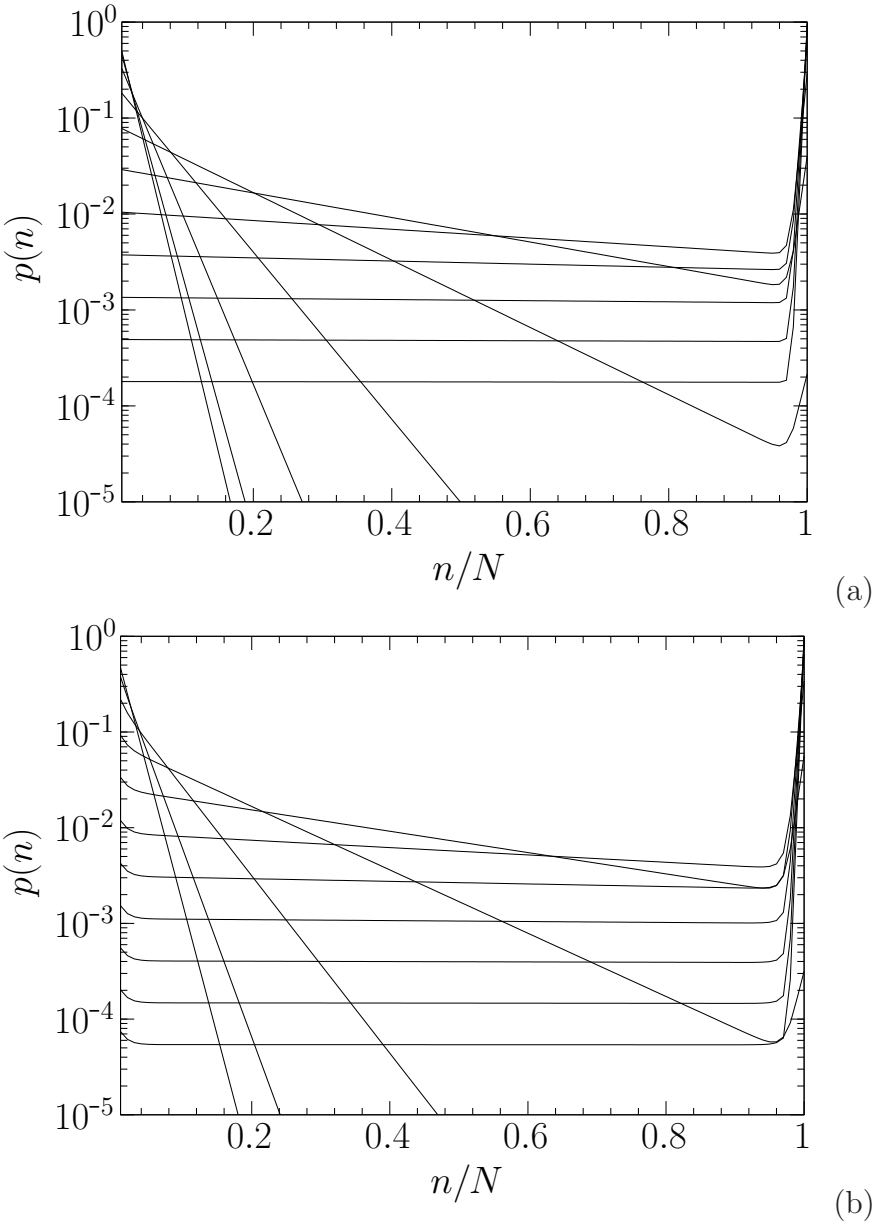

Figure 3. Cluster distribution $p(n)$ of $N = 100$ particles, for $K_0 = 5$ and (a) $h = 0$ and (b) $h = 0.5$, obtained from Eq. (12). Eleven curves, from top to bottom along the vertical axis at $n/N = 0$, correspond to the cases $K = 0$ to 5 at the increment of 0.5, i.e., $K = 0$, 0.5, 1, 1.5, $\cdots$, 5.

$v^* \approx 1$. In this case, asymptotic calculations give $\ln(2\cosh K) - S_0^*(0) \approx -1/\cosh(K)^2$; this in turn leads to

$$p(N) \approx \exp[-\mathrm{e}^{-2K+\ln(4N)}] \tag{22}$$

which is identified as a universal cumulative Gumbel distribution for the largest occupancy $n = N$, in terms of the energy excitation $2J$ and the corresponding entropy increase $\ln(4N)$. Note that there are $4N$ accessible states because both $\mathcal{S}_{1D}$ and $\mathcal{S}_C$ are symmetric under the transformation $\sigma_i \to -\sigma_i$. Numerical computation of $p(N)$ directly

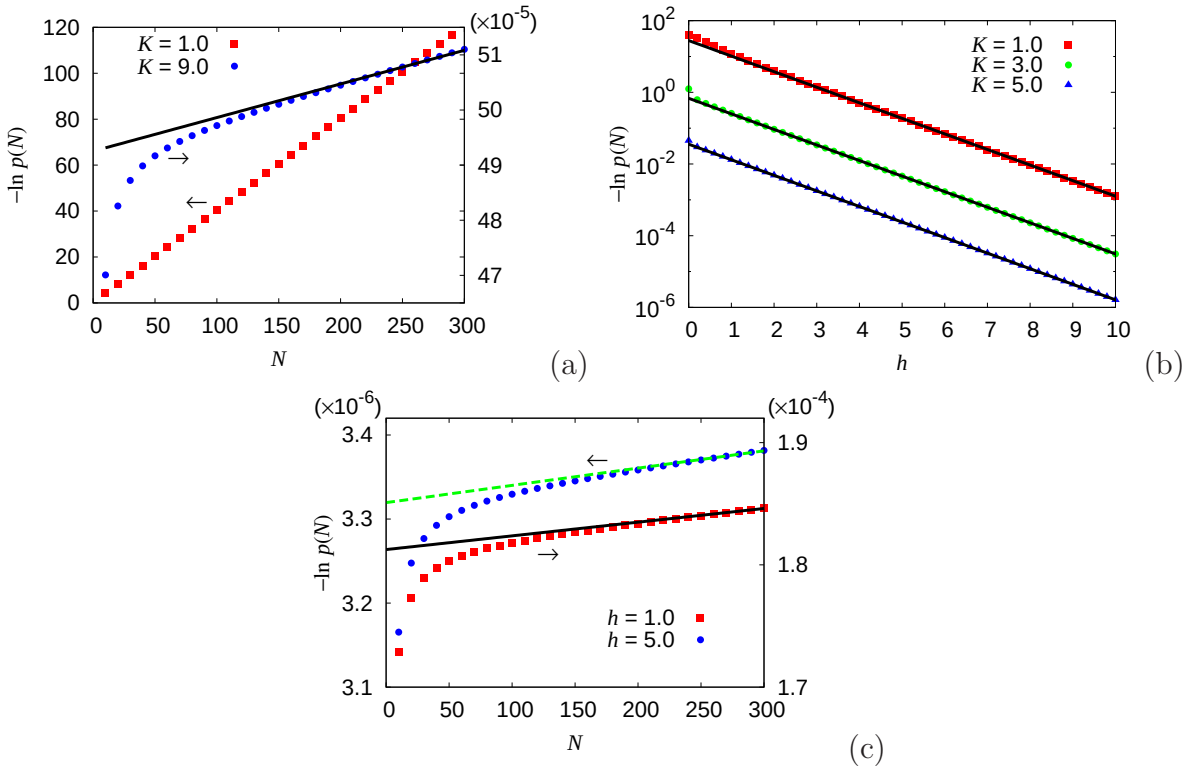

Figure 4. Asymptotic behavior of the maximum occupancy probability $p(N)$ for $K_0 = 1$. (a) $-\ln p(N)$ versus the number N of particles in the absence of the field. Red squares and blue circles represent the numerical results from the exact relation $p(N) = W_N/Z_0$ for $K = 1$ and $K = 9$, respectively. The linear relation is verified for most values of N when K is small ($K = 1$). This agrees with Eq. (21) which indicates the relation $-\ln p(N) \sim N \ln 2$ for K near zero. For a large value of K ($= 9$), the linear relation is still valid for N large; numerical results indeed agree well with equation Eq. (22) (black solid line), $-\ln p(N) \sim 4\mathrm{e}^{-2K} N \approx 6 \times 10^{-8} N$. (b) $-\ln p(N)$ versus the external field h in the system of $N = 100$ particles. Irrespective of K, the linear relations with slope -1 (black solid lines) are clearly verified, which is supportive of Eq. (23). The small jump of $-\ln p(N)$ at $h = 0$ reflects the dependence on N between Eqs. (22) and (23). The behavior of $p(N)$ in both (a) and (b) hardly alters even if other values of K_0 are used. (c) $-\ln p(N)$ versus N in the presence of the field. Red squares and blue circles represent the exact numerical results for $h = 1$ and $h = 5$, respectively. For large N, the linear relation is apparent. Furthermore, the slopes of the black solid (for $h = 1$) and green dashed (for $h = 5$) lines computed from Eq. (23) agree well with the numerical results. It is thus confirmed that the entropic contribution to the free energy should be modified under the external field.

from the exact relation $p(N) = W_N/Z_0$ also confirms the expression in Eq. (22) in the thermodynamics limit ($N \to \infty$), as shown in Fig. 4(a). We also note that Eqs. (18) and (19) as well as Eq. (22) are free from K_0, for we are considering the paramagnetic sector in which $\mathcal{S}_C$ is disordered.

We now consider the system in the presence of the external field h. As for it, one may attempt to obtain the asymptotic expression of the distribution, utilizing the relations in Appendices A and B. Here, rather than performing such formidable calculations, we

instead carry out numerical summations which take less effort but still provide results sufficient to investigate the dependence of $p(N)$ on the external field h. As shown clearly in Fig. 4(b), numerical computation leads to the relation $-\ln p(N) \propto \mathrm{e}^{-h}$ and we speculate here that the maximum occupancy probability $p(N)$ in the presence of the field takes the form

$$p(N) \approx \exp[-\mathrm{e}^{-2K-h+\ln(2N)}]. \tag{23}$$

Consistently with Eq. (22), one may confirm that the argument is given by the free energy cost to remove one particle from $\mathcal{S}_{1D}$. Specifically, the term $2J + h_e$ represents the energy of removing one particle. Meanwhile, Fig. 4(c) manifests that the entropic contribution to the free energy should be modified from $\ln(4N)$ to $\ln(2N)$, reflecting the reduced number of accessible states due to the explicitly broken symmetry of $\mathcal{S}_{1D}$ under the nonzero external field. Defining the free energy cost $\Delta F \equiv 2J + h_e - T\ln(2N)$, we then conclude that the probability distribution for the maximum occupancy $p(N)$ in the presence of the field is also given by a cumulative Gumbel distribution $p(N) = \exp(-\mathrm{e}^{-x})$ with the argument $x = \Delta F/T$.

In addition, Fig. 5, which displays $p(N)$ versus K obtained from $p(N) = W_N/Z_0$, discloses a crossover between the two regimes: $p(N)$ close to unity and $p(N)$ close to zero. In fact, $p(N)$ should vanish in the thermodynamic limit and indeed approaches zero for given N as K decreases below $K^* \approx \frac{1}{2}\ln(4N)$ which is a characteristic value of Eq. (22). In the case $K > K^*$, however, N is not large enough for the system to enter the regime of the thermodynamic limit and $p(N)$ deviates from Eq. (22), approaching unity. Note here that the value of K^* depends rather weakly (logarithmically) on N. For given N, therefore $p(N)$ is expected to change from zero to unity as K is raised [see Fig. 5(a)]. In this sense, we conclude that there appears a crossover behavior around the crossover coupling K^*. Numerical results for $N = 100$, shown in Fig. 5(b), indeed demonstrate the crossover behavior: While $-\ln p(N)$ follows Eq. (22) well in the region $1 \lesssim K \lesssim 3$, clear discrepancies between the asymptotic relation and numerical results are observed for $K \gtrsim 3$. Note that the crossover coupling in this case ($N = 100$) is given by $K^* \approx 3$. This crossover behavior persists also in the presence of the field, as presented in Fig. 5(c).

4. Model with fugacity

Instead of the particle exchange with system $\mathcal{S}_C$, we now consider the system specified by constant fugacity $z_0 = \exp(\mu/k_BT)$ such that $V = 2z_0$, where μ is the chemical potential. In this case we have $z_N(s) = (2z_0)^{N-s}$. It is an approximation of the previous model where the function $V = V(y)$ is replaced by an average constant value, or more specifically where the chemical potential is constant. In the absence of the external field, the action S_0 is similar in the continuum limit to Eq. (15) and is expressed as

$$\begin{aligned} S_0(x) &= \ln 2 + (v-u)\ln\cosh K + (1-v)\ln z_0 \\ &- 2u\ln u + (v-x)\ln(v-x) + (1-v)\ln(1-v) \end{aligned}$$

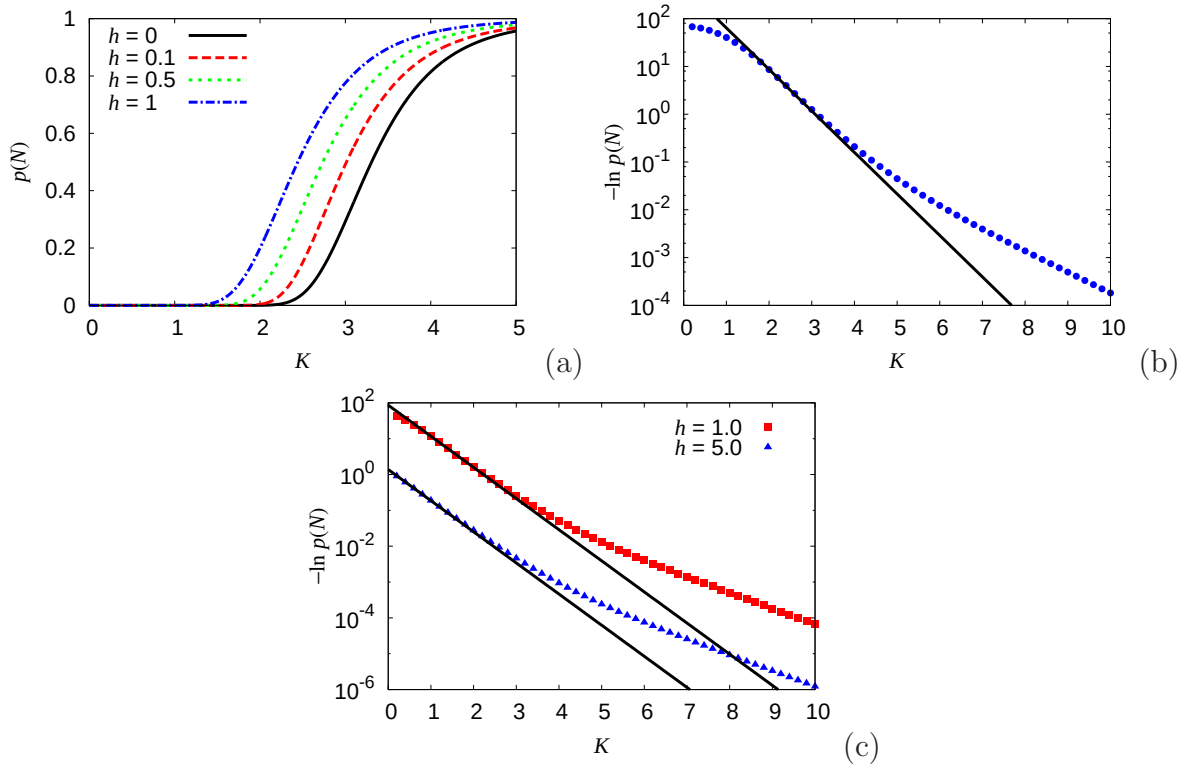

Figure 5. Crossover behavior in the system of $N = 100$ particles with respect to K. (a) Probability $p(N)$ that the system $\mathcal{S}_{1D}$ is fully occupied, computed from the exact relation. Dependence on coupling K is displayed, for $K_0 = 5$ and various strengths of the field h. In general the probability increases with the field, as expected. The crossover between $p(N)$ close to unity and to zero is also manifested. (b) $-\ln p(N)$ versus K in the absence of the field. Blue circles show the results for $K_0 = 1$ while the black solid line, carrying the slope -2 in the semi-logarithmic scale, represents the double exponential decay in Eq. (22). Here the crossover is observed near $K^* = \frac{1}{2}\ln(4N) \approx 3.0$ (see text), beyond which the dependence of $p(N)$ on K deviates from Eq. (22). (c) $-\ln p(N)$ versus K in the presence of the field $h = 1$ (red squares) and $h = 5$ (blue triangles) for $K_0 = 1$. As in the case of $h = 0$, numerical results follow the double exponential decay in Eq. (23) (represented by the solid lines) up to $K = K^*$; discrepancies are obvious beyond K^*, again demonstrating a crossover. As expected, results in all cases hardly alter even if other values of K_0 are used.

$$-(v-u-x)\ln(v-u-x)-(1-u-v)\ln(1-u-v). \tag{24}$$

The saddle point is specified by the set of equations

$$\begin{aligned}\cosh K &= \frac{(v-u-x)(1-u-v)}{u^2}\\ \frac{\cosh K}{z_0} &= \frac{(1-v)(v-u-x)}{(v-x)(1-u-v)}\end{aligned} \tag{25}$$

whose solutions are given by

$$u^* = \frac{2(1-x)z_0}{\sqrt{(\cosh K - z_0)^2+4z_0}\left[\cosh K + z_0 + \sqrt{(\cosh K - z_0)^2+4z_0}\right]}$$

$$v^* = \frac{1}{2}\left[1 + x + (1-x)\frac{\cosh K - z_0}{\sqrt{(\cosh K - z_0)^2 + 4z_0}}\right]. \tag{26}$$

From these, the asymptotic limit of $p(n)$ in Eq. (13) or $p(x)$ for $x < 1$ is described by the saddle-point approximation

$$p(x) = C_x \exp\left(N[S_0^*(x) - S_0^*(0)]\right) \tag{27}$$

with

$$C_x = \frac{2z_0}{\cosh K\left[\sqrt{(\cosh K - z_0)^2 + 4z_0} + \cosh K - z_0\right]}$$

where the extremal value $S_0^*(x)$ is given by Eq. (24) with u and v replaced by Eq. (26). One may consider two limits: K is sufficiently larger or smaller than unity. In these two limits, the distribution takes the form:

$$\begin{aligned} p(x) &\approx 4z_0 \exp\left[-2K - 4z_0 N \mathrm{e}^{-2K} x\right],\ K \gg 1 \\ p(x) &\approx z_0 \exp\left[-N\ln(1+z_0)x\right],\ K \ll 1. \end{aligned} \tag{28}$$

In Fig. 6, we plot $p(n)$ computed from Eq. (12) for several values of K. It is also shown that Eq. (27) fits well the discrete sum, e.g., for $K = 2$ and 5. The saddle-point solution for $p(N)$ is instead given by Eq. (21) with S_0 and (u^*, v^*) replaced by Eqs. (24) and (26), respectively, with $x = 0$:

$$p(N) = C_N \exp\left(N[\ln(2\cosh K) - S_0^*(0)]\right) \tag{29}$$

with

$$C_N = \frac{4z_0\sqrt{(\cosh K - z_0)^2 + 4z_0}}{\cosh K\left[\left(\sqrt{(\cosh K - z_0)^2 + 4z_0} + z_0\right)^2 - \cosh^2 K\right]}.$$

Making use of the asymptotic expansion of the argument in Eq. (29),

$$\ln(2\cosh K) - S_0^*(0) \approx -\frac{z_0}{\cosh^2 K} + \frac{z_0^2}{\cosh^4 K} \tag{30}$$

and the coefficient $C_N \approx 1$, we obtain

$$p(N) \approx \exp\left[-\mathrm{e}^{-2K + \ln(2z_0) + \ln(2N)}\right] \tag{31}$$

which becomes vanishingly small for K lower than the crossover value $K^* = \frac{1}{2}\ln(4z_0 N)$.

In the absence of the field, the saddle-point solution in Eq. (21) is in perfect agreement with the exact discrete summation. In the limit $x \to 1$, the arguments of the exponential in $p(x)$ and $p(N)$ coincide, to the leading order in N, with each other since

$$\lim_{x\to 1} S_0^*(x) = \ln(2\cosh K). \tag{32}$$

It is shown in Fig. 6 that this saddle-point approximation for $x \neq 1$ does work well around $x = 1$, as $p(x)$ should approach $p(N)$. The particular solution $C_x = C_N$ is given by $K = \cosh^{-1}(z_0^{2/3} - z_0^{1/3} + z_0)$ for $z_0 > 1$, which leads to $\lim_{x\to 1} p(x) = p(N)$. Further, in the presence of the field, the discrete sum for $p(N)$ given by Eq. (12) can be evaluated in the case of a constant fugacity, and the results are displayed in Fig. 7.

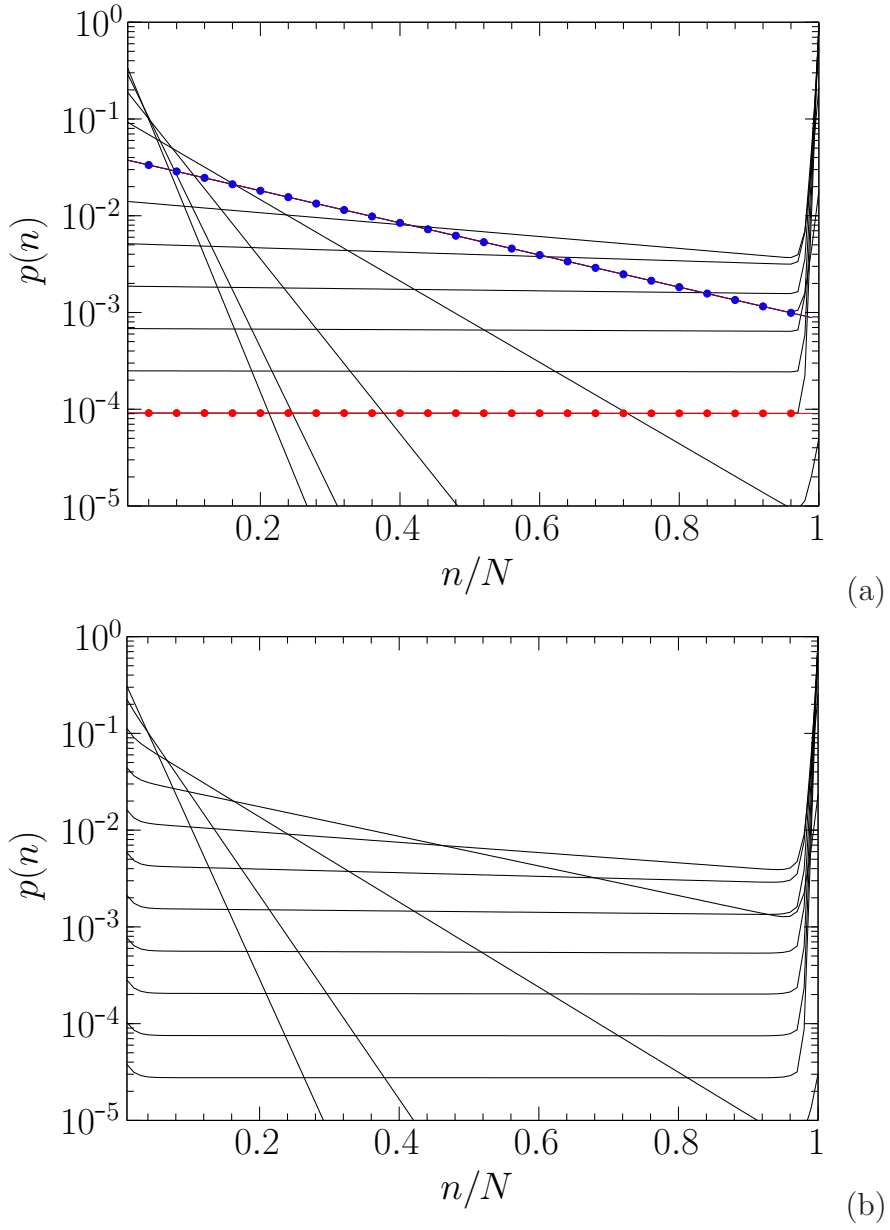

Figure 6. Cluster distribution $p(n)$ of $N = 100$ particles, obtained from Eq. (12), for fugacity $z_0 = 0.5$ and field $h =$ (a) 0 and (b) 0.5. Eleven curves, from top to bottom along the vertical axis at $n/N = 0$, correspond to the cases $K = 0$ to 5 at the increment of 0.5, i.e., $K = 0$, 0.5, 1, 1.5, $\cdots$, 5. The saddle-point solution in Eq. (27) for $h = 0$ is plotted by the blue and red circles for $K = 2$ and 5, respectively. Good agreement with the numerical results is observed.

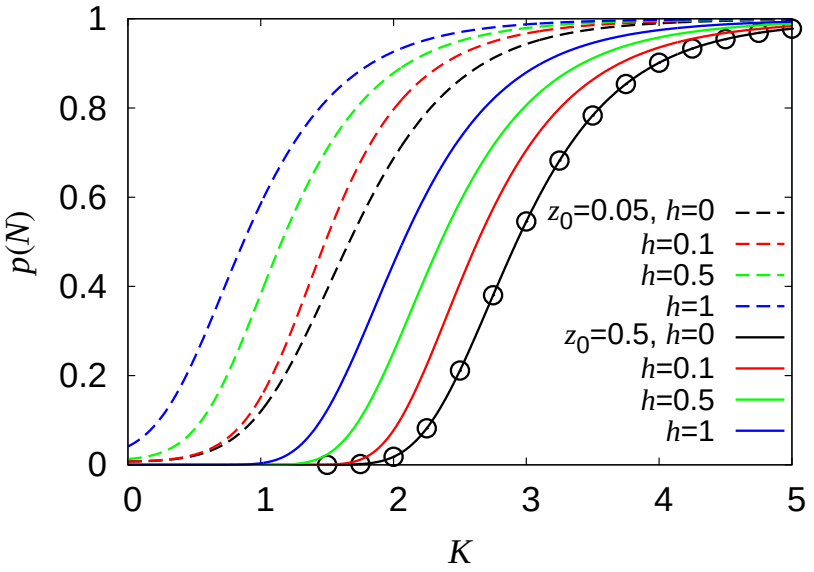

Figure 7. Probability $p(N)$ versus coupling K, for $N = 100$ and various values of the fugacity z_0 and field h. The saddle-point solution in Eq. (29) for $z_0 = 0.5$ and $h = 0$ is plotted by circles and fits well the numerical sum given by Eq. (12).

5. Conclusion

We have studied statistical mechanics of particle exchanges in two different systems, between which no direct interactions are present. This provides a model for the evaporation process which occurs between two media, one being a one-dimensional ordered lattice. It is found that the probability $p(N)$ of maximum occupation in $\mathcal{S}_{1D}$ follows a universal cumulative Gumbel distribution, with argument being proportional to the free energy cost to remove one particle, which has been obtained by identifying the energy and entropy of such an excitation in the presence of an external field. Gumbel distribution is usually found in the field of extreme-value statistics [14, 15], and represents the distribution of the extreme values of a set of independent and identically distributed random variables. Here $\mathcal{S}_C$ is a fully-connected system, simulating a gas or a reservoir with a uniform chemical potential; both cases display similar characteristics and an identical universal distribution. Specifically, $p(N)$ can be computed via the saddle-point analysis and presents a crossover in relation to a first-order transition from $y^* = 0$ to a finite value.

We expect that the formulation incorporating two systems and their particle exchanges may serve as a framework to probe various phenomena in complex systems in new perspectives. For example, one may attempt to improve growth models, in which elements can be added or eliminated [16, 17, 18, 19], by specifying the particle exchange mechanism as well as such characteristics as the dimensionality of the system and environment. In this way, the relevance of the model to physical systems could be strengthened; this is left for future study.

Acknowledgments

This work was supported by the National Research Foundation of Korea through the Basic Science Research Program (Grant No. 2016R1D1A1A09917318).

Author contribution statement

J.-Y. Fortin and M.Y. Choi contributed to the development of the project and theoretical model. J.-Y. Fortin and S. Goh performed the calculations and C. Kim assisted numerical analysis. All authors contributed to the writing of the manuscript and discussion of the obtained results.

Appendix A. Cluster combinatorial

Here we compute the sum of all k-cluster contributions of size n_i under the constraint $s = n_1 + \cdots + n_k$. We use the complex integral representation of the Kronecker delta:

$$\omega_k(s) = \sum_{n_1,n_2,\cdots n_k \geq 1} W_{n_1} W_{n_2} \cdots W_{n_k} \delta_{s,n_1+\cdots+n_k} = \oint \frac{\mathrm{d}z}{2i\pi z} z^s \left(\sum_{n=1}^{\infty} z^{-n} W_n \right)^k \tag{A.1}$$

where W_n is the weight of an n-spin cluster with open boundaries. It is defined by the product

$$W_n = \left\langle v^{\mathsf{T}} \hat{W}^{n-1} v \right\rangle = r_+ \lambda_+^{n-1} + r_- \lambda_-^{n-1}. \tag{A.2}$$

$\hat{W}$ is the transfer matrix and v the boundary vector

$$\hat{W} = \begin{pmatrix} \mathrm{e}^{K+h} & \mathrm{e}^{-K} \\ \mathrm{e}^{-K} & \mathrm{e}^{K-h} \end{pmatrix} \quad \text{and} \quad v = \begin{pmatrix} \mathrm{e}^{h/2} \\ \mathrm{e}^{-h/2} \end{pmatrix}. \tag{A.3}$$

The eigenvalues $\lambda_\pm$ and coefficients $r_\pm$ are given by

$$\begin{aligned} \lambda_\pm &= \mathrm{e}^K \cosh h \pm \sqrt{\mathrm{e}^{2K} \sinh^2 h + \mathrm{e}^{-2K}} \\ r_+ &= \frac{(e^{h/2} + \alpha \mathrm{e}^{-h/2})^2}{1+\alpha^2} \\ r_- &= \frac{(e^{h/2}\alpha - \mathrm{e}^{-h/2})^2}{1+\alpha^2} \end{aligned} \tag{A.4}$$

with

$$\alpha = \sqrt{1 + \mathrm{e}^{4K} \sinh^2 h} - \mathrm{e}^{2K} \sinh h$$

which reduce in the absence of the field to $\lambda_+ = 2\cosh K$, $\lambda_- = 2\sinh K$, $r_+ = 2$, and $r_- = 0$. The complex integral in Eq. (A.1) is then evaluated by summing the series over n:

$$\begin{aligned} \omega_k(s) &= \oint \frac{\mathrm{d}z}{2i\pi z} z^s \left(\frac{r_+}{z-\lambda_+} + \frac{r_-}{z-\lambda_-} \right)^k \\ &= \oint \frac{\mathrm{d}z}{2i\pi} \sum_{l=0}^{k} \binom{k}{l} r_+^l r_-^{k-l} \frac{z^{s-1}}{(z-\lambda_+)^l (z-\lambda_-)^{k-l}}. \end{aligned}$$

The contour integral encloses two eigenvalues and therefore the two residues at $z = \lambda_\pm$ should be computed separately by performing successive differentiations with respect to z of the integrand. After some algebra, one obtains

$$\omega_k(s) = \sum_{l=0}^{k} \binom{k}{l} r_+^l r_-^{k-l} \left[\sum_{m=0}^{l-1} \binom{s-1}{m} \binom{k-m-2}{l-m-1} (-1)^{l-1-m} \frac{\lambda_+^{s-m-1}}{(\lambda_+ - \lambda_-)^{k-m-1}} \right.$$
$$\left. + \sum_{m=0}^{k-l-1} \binom{s-1}{m} \binom{k-m-2}{l-1} (-1)^{l} \frac{\lambda_-^{s-m-1}}{(\lambda_+ - \lambda_-)^{k-m-1}} \right]. \tag{A.5}$$

It is understood in the different sums that if one binomial coefficient has a negative argument, it is set equal to zero unless both arguments are equal, in which case it is unity. In particular, the term $l = 0$ in the sum is equal to $r_-^k \binom{k-1}{s-1} \lambda_-^{s-k}$ and $r_+^k \binom{k-1}{s-1} \lambda_+^{s-k}$ for $l = k$.

Appendix B. Thermodynamic limit

The thermodynamic limit of Eq. (13) can be obtained by rescaling the variables $x = n/N$, $u = k/N$, and $v = s/N$. This leads to a triple integral involving a continuous action $S_0(x)$. In particular, we use the expansion of the gamma function:

$$\ln \Gamma(Na + b) \approx aN \ln N + (a \ln a - a)N + \left(b - \frac{1}{2}\right) \ln N$$
$$+ \left(b - \frac{1}{2}\right) \ln a + \frac{1}{2} \ln(2\pi).$$

The expression for $p(n)$ in Eq. (13) involves three binomial coefficients. The first term can be expressed with gamma functions

$$\binom{N-s+1}{N-s-k+1} = \frac{\Gamma(N-s+2)}{\Gamma(N-s-k+2)\Gamma(k+1)}$$
$$= \frac{\Gamma(N(1-v)+2)}{\Gamma(N(1-u-v)+2)\Gamma(Nu+1)}$$

and this is approximately equal to

$$\binom{N-s+1}{N-s-k+1} \approx \tag{B.1}$$
$$\exp\left[N\left\{(1-v)\ln(1-v) - u\ln u - (1-u-v)\ln(1-u-v)\right\}\right.$$
$$\left. - \frac{1}{2}\ln N + \frac{3}{2}\ln(1-v) - \frac{3}{2}\ln(1-u-v) - \frac{1}{2}\ln u - \frac{1}{2}\ln(2\pi)\right].$$

The second term is given by

$$\binom{s-n-1}{k-2} = \frac{\Gamma(N(v-x))}{\Gamma(Nu-1)\Gamma(N(v-u-x)+2)}$$
$$\approx \exp\left[N\left\{(v-x)\ln(v-x) - u\ln u - (v-u-x)\ln(v-u-x)\right\}\right]$$
$$\times \exp\left[-\frac{1}{2}\ln N \frac{3}{2}\ln u - \frac{3}{2}\ln(v-u-x) - \frac{1}{2}\ln(v-x) - \frac{1}{2}\ln(2\pi)\right]. \tag{B.2}$$

Finally, the last binomial coefficient can be approximated by

$$\begin{aligned}\binom{s-1}{k-1} &= \frac{\Gamma(Nv)}{\Gamma(Nu)\Gamma(N(v-u)+1)} \\ &\approx \exp\left[N\left[v\ln v-(v-u)\ln(v-u)-u\ln u\right]-\frac{1}{2}\ln N\right] \\ &\times \exp\left[\frac{1}{2}\ln u-\frac{1}{2}\ln(v-u)-\frac{1}{2}\ln v-\frac{1}{2}\ln(2\pi)\right]. \end{aligned} \tag{B.3}$$

References

[1] Paul M Chaikin and Tom C Lubensky. *Principles of Condensed Matter Physics*. Cambridge Univ Press, Cambridge, 2000.

[2] Rodney J Baxter. *Exactly Solved Models in Statistical Mechanics*. Academic Press, London, 1989.

[3] J. Marro and R. Dickman. *Nonequilibrium Phase Transitions in Lattice Models*. Cambridge University Press, Cambridge, 1999.

[4] G. Oshanin, O. Bénichou, and A. Blumen. Exactly solvable model of reactions on a random catalytic chain. *J. Stat. Phys.*, 112(3):541–586, 2003.

[5] Andrew N. Jordan, C. H. Raymond Ooi, and Anatoly A. Svidzinsky. Fluctuation statistics of mesoscopic bose-einstein condensates: Reconciling the master equation with the partition function to reexamine the uhlenbeck-einstein dilemma. *Phys. Rev. A*, 74:032506, Sep 2006.

[6] Anatoly A. Svidzinsky and Marlan O. Scully. Condensation of n bosons: Microscopic approach to fluctuations in an interacting bose gas. *Phys. Rev. A*, 82:063630, Dec 2010.

[7] Zoltán Rácz. Aggregation in the presence of sources and sinks: A scaling theory. *Phys. Rev. A*, 32:1129–1133, Aug 1985.

[8] Colm Connaughton, R Rajesh, and Oleg Zaboronski. On the non-equilibrium phase transition in evaporation–deposition models. *J. Stat. Mech.: Theor. Exp.*, 2010(09):P09016, 2010.

[9] Jean-Yves Fortin. Crossover properties of a one-dimensional reaction-diffusion process with a transport current. *J. Stat. Mech.: Theor. Exp.*, 2014(9):P09033, 2014.

[10] Daniel ben Avraham, Martin A. Burschka, and Charles R. Doering. Statics and dynamics of a diffusion-limited reaction: Anomalous kinetics, nonequilibrium self-ordering, and a dynamic transition. *J. Stat. Phys.*, 60(5):695–728, 1990.

[11] A.P. Masucci, J. Serras, A. Johansson, and M. Batty. Gravity versus radiation models: On the importance of scale and heterogeneity in commuting flows. *Phys. Rev. E*, 88:022812, 2013.

[12] Segun Goh, Jean-Yves Fortin, and MooYoung Choi. Phase transitions and relaxation dynamics of ising models exchanging particles. *Physica A*, 466:166 – 179, 2017.

[13] Nigel Goldenfeld. *Lectures on Phase Transitions and the Renormalization Group*. Addison-Wesley, Urbana-Champaign, 1992.

[14] Jan Beirlant, Yuri Goegebeur, Johan Segers, and Jozef Teugels. *Statistics of Extremes: Theory and Applications*. Wiley, Chichester, 2004.

[15] Jean-Yves Fortin and Maxime Clusel. Applications of extreme value statistics in physics. *J. Phys. A*, 48(18):183001, 2015.

[16] M.Y. Choi, H. Choi, J.-Y. Fortin, and J. Choi. How skew distributions emerge in evolving systems. *Europhys. Lett.*, 85:30006, 2009.

[17] S. Goh, H. W. Kwon, M.Y. Choi, and J.-Y. Fortin. Emergence of skew distributions in controlled growth processes. *Phys. Rev. E*, 82:061115, Dec 2010.

[18] Jean-Yves Fortin, Sophie Mantelli, and MooYoung Choi. Dynamics of interval fragmentation and asymptotic distributions. *J. Phys. A*, 46(22):225002, 2013.

[19] S. Goh, H. W. Kwon, and M.Y. Choi. Discriminating between weibull distributions and log-normal distributions emerging in branching processes. *J. Phys. A*, 47(22):225101, 2014.